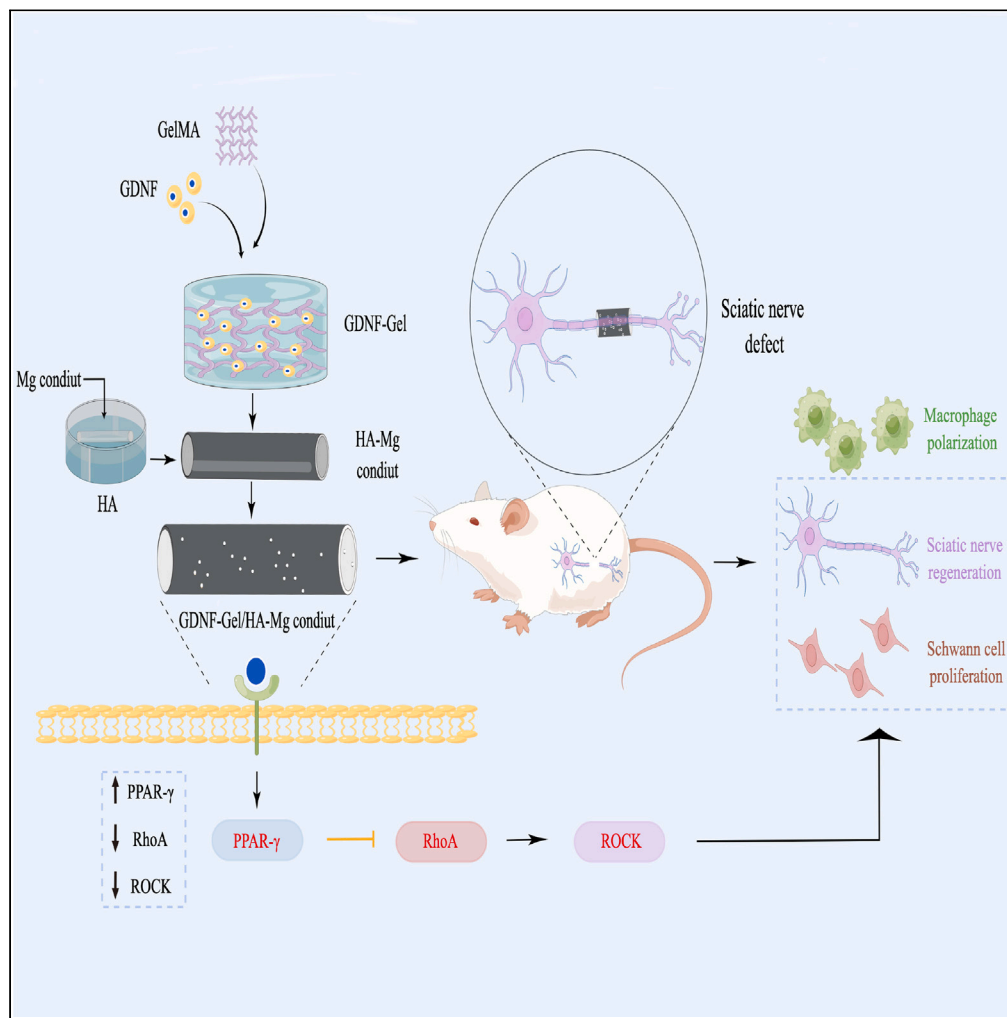


Article

The GDNF-gel/HA-Mg conduit promotes the repair of peripheral nerve defects by regulating PPAR- γ /RhoA/ROCK signaling pathway



Yuanqing Cai, Yi Chen, Guangyang Zhang, ..., Yong Wang, Xinyu Fang, Xiaoqian Dang

yongwangcqu_1968@163.com (Y.W.)
fangxinyu0417@fjmu.edu.cn (X.F.)
dangxiaoqian@xjtu.edu.cn (X.D.)

Highlights

GDNF-Gel/HA-Mg conduits improve corrosion resistance of Mg

GDNF-Gel/HA-Mg conduits could promote peripheral nerve defects repair

GDNF-Gel/HA-Mg conduits could improve nerve repair related genes expression

GDNF-Gel/HA-Mg conduits regulate PPAR- γ /RhoA/ROCK pathway in peripheral nerve repair

Cai et al., iScience 27, 108969
February 16, 2024 © 2024 The Author(s).
<https://doi.org/10.1016/j.isci.2024.108969>



Article

The GDNF-gel/HA-Mg conduit promotes the repair of peripheral nerve defects by regulating PPAR- γ /RhoA/ROCK signaling pathway

Yuanqing Cai,^{1,6} Yi Chen,^{2,6} Guangyang Zhang,¹ Yi Lin,³ Jianan Zhang,⁴ Jialin Liang,¹ Leifeng Lv,¹ Yong Wang,^{2,*} Xinyu Fang,^{5,*} and Xiaoqian Dang^{1,7,*}

SUMMARY

Magnesium (Mg)-based conduits have gained more attention in repairing peripheral nerve defects. However, they are limited due to poor corrosion resistance and rapid degradation rate. To tackle this issue, glial cell line-derived neurotrophic factor (GDNF)- Gelatin methacryloyl (Gel)/hydroxylapatite (HA)-Mg nerve conduit was developed and implanted in sciatic nerve defect model in Sprague-Dawley (SD) rats. The sciatic functional index measurement showed that the GDNF-Gel/HA-Mg nerve conduit effectively promoted the recovery of sciatic nerve function. The pathological examination results showed that there were more regenerated nerve tissues in GDNF-Gel/HA-Mg group, with a higher number of regenerating axons, and the thickness of the myelin sheath was significantly larger than that of control group (NC group). Immunofluorescence results revealed that the GDNF-Gel/HA-Mg conduit significantly promoted the expression of genes associated with nerve repair. RNA-seq and molecular test results indicated that GDNF-Gel/HA-Mg might be involved in the repair of peripheral nerve defects by regulating PPAR- γ /RhoA/ROCK signaling pathway.

Biological sciences; Neuroscience; Molecular neuroscience; Techniques in neuroscience

INTRODUCTION

Peripheral nerve injury (PNI) is a common clinical disease, often caused by trauma, leading to severe complications such as dysfunction of target organs and muscle atrophy, imposing a heavy burden on individuals and society.¹ In cases of mild PNI where the nerve remains intact, surgical intervention is usually not required, and nerve nutrition support is an effective treatment that could promote the restoration of normal nerve function.^{1,2} However, in cases of severe PNI with nerve defects, surgical intervention is necessary. The fundamental principle in treating peripheral nerve defects is to reinstate the continuity of the nerve. In cases of small nerve defects, the direct end-to-end suturing technique can be employed to repair the defects. However, for longer gaps in the nerve, autologous nerve transplantation is widely regarded as the most effective method.² Nonetheless, it is important to acknowledge that autologous nerve transplantation has certain limitations, including additional surgical trauma, scarring and sensory impairments in the donor area, pain in donor area caused by neuroma, and mismatched nerve structures between the donor and recipient areas.¹⁻³ These limitations impose constraints on the clinical promotion and application of autologous nerve transplantation.

Currently, artificially fabricated nerve conduits have emerged as a highly promising approach for the treatment of peripheral nerve defects.⁴⁻⁶ These conduits are capable of replicating the growth conditions observed in autologous nerve transplantation and creating a micro-environment conducive to cell proliferation, nerve and axonal regeneration.⁶⁻⁸ This fascinating and challenging research field has garnered increasing interest and attention from medical professionals and materials scientists. However, despite numerous researches have attempted to utilize various types of nerve conduits for nerve defect repair, regrettably, these nerve conduits often exhibit limitations such as conduit collapse, poor regeneration, excessive scar tissue formation and adhesion, immune reactions and immunosuppression, as well as the complexity in manufacturing processes, etc., thus, the repair effects remain unsatisfactory.^{7,9-11} An ideal nerve conduit for peripheral nerve defect repair should possess the following characteristics^{6,8,12}: firstly, it should exhibit excellent biocompatibility and biodegradability, with a controllable degradation rate that matches the pace of neural growth, while ensuring non-toxic degradation products. Secondly, it should

¹Department of Orthopaedics, The Second Affiliated Hospital of Xi'an Jiaotong University, Xi'an 710006, China

²College of Materials Science & Engineering, National Engineering Research Center for Magnesium Alloys, Chongqing University, Chongqing 400045, China

³Department of Ophthalmology, The Third Affiliated Hospital of Chongqing Medical University, Chongqing 401120, China

⁴Zonglian College, Xi'an Jiaotong University, Xi'an 710054, China

⁵Department of Orthopaedic Surgery, the First Affiliated Hospital, Fujian Medical University, Fuzhou 350005, China

⁶These authors contributed equally

⁷Lead contact

*Correspondence: yongwangcqu_1968@163.com (Y.W.), fangxinyu0417@fjmu.edu.cn (X.F.), dangxiaoqian@xjtu.edu.cn (X.D.)
<https://doi.org/10.1016/j.isci.2024.108969>



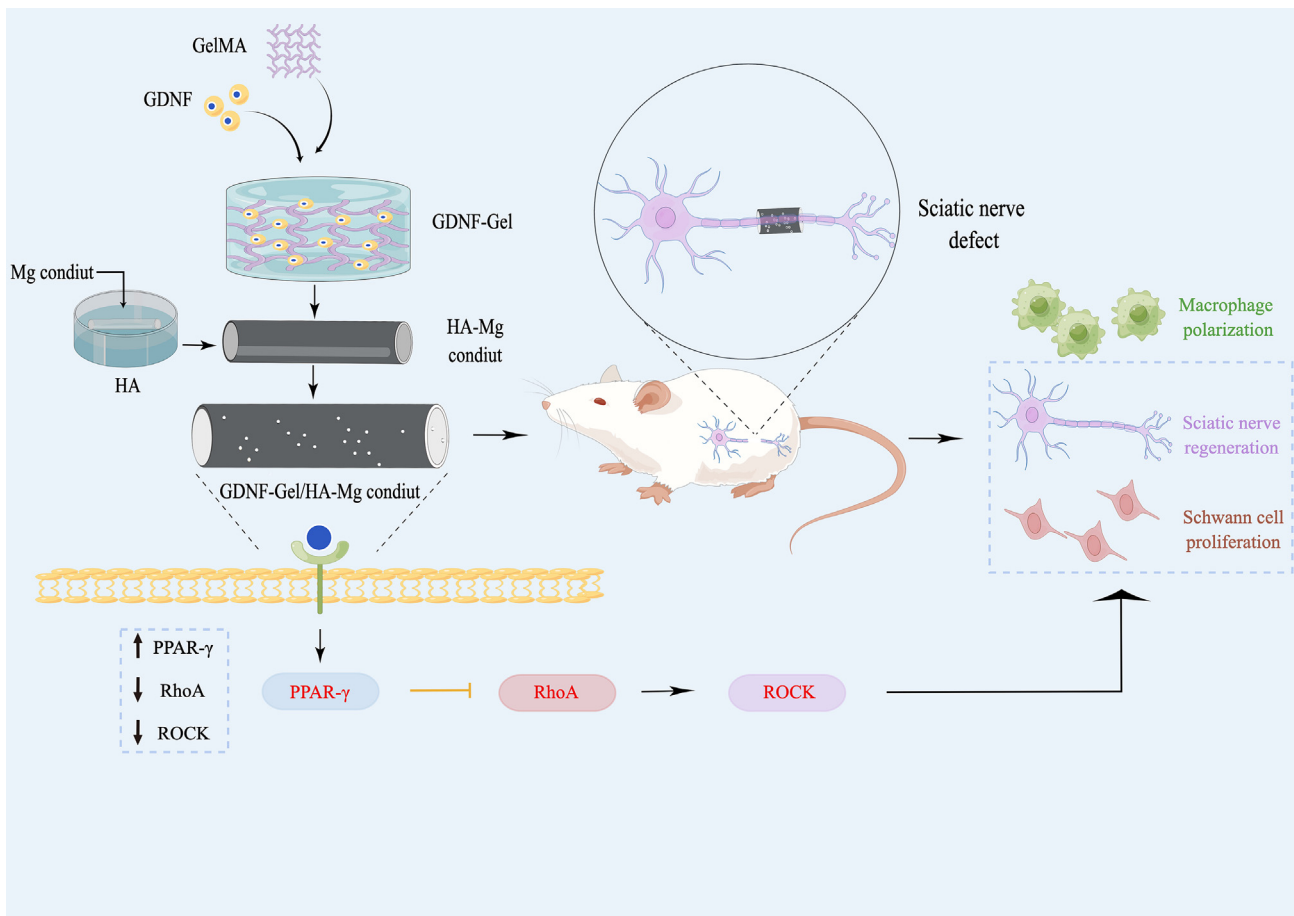


Figure 1. Graphic abstract: the preparation of GDNF-Gel/HA-Mg conduit and its potential value in repairing peripheral nerve defect

Mg, magnesium; HA, hydroxyapatite; GDNF, glial cell line-derived neurotrophic factor; GelMA, Gelatin methacryloyl; PPAR- γ , peroxisome proliferator-activated receptor gamma; ROCK, Rho-associated kinase.

facilitate and promote axonal growth, while also possessing appropriate mechanical properties to facilitate surgical implantation. Additionally, peripheral nerves release growth factors during self-repair to promote axonal regeneration, and it is feasible to incorporate neurotrophic factors into nerve conduits, simulating the process of growth factor released by neurons after PNI, thereby providing sustained nourishment for neuronal and axonal regeneration.

Magnesium (Mg)-based nerve conduits are highly desirable in peripheral nerve defect repair due to their exceptional biocompatibility and biodegradability.^{5,13} The degradation process of magnesium-based nerve conduits could produce magnesium ion (Mg^{2+}), which is one of essential elements for the human body and are non-toxic.¹⁴ Researches also have demonstrated that Mg^{2+} can effectively promote the regeneration of peripheral nerves.^{13,15} Moreover, Mg-based nerve conduits exhibit favorable mechanical properties that provide support and guidance for nerve regrowth.¹³ Nevertheless, there are limitations associated with Mg-based nerve conduits that impede their further promotion and application. On one hand, magnesium-based nerve conduits have poor corrosion resistance, its degradation rate is relatively fast and does not match the growth rate of peripheral nerves.¹³ On the other hand, the rapid degradation and release of hydrogen could affect the pH value of the microenvironment, which is unfavorable for nerve tissue regeneration.¹³

To address these issues, this study employed a liquid-phase deposition method to modify magnesium with a hydroxyapatite (HA) coating, namely, HA-Mg enhancing its corrosion resistance. Glial cell line-derived neurotrophic factor (GDNF), a member of the transforming growth factor β superfamily, previous studies have demonstrated its efficacy in promoting axonal regeneration, Schwann cell migration, and myelin sheath production.^{16–18} Therefore, in this study, Gelatin methacryloyl (GelMA) was used for loading and sustained release of GDNF, which was then combined with the HA-Mg nerve conduit to create the GDNF-Gel/HA-Mg nerve conduit, aiming to enhance the nutritional support required for peripheral nerve regeneration. Afterward, a sciatic nerve defect model was established to investigate the role and molecular mechanism of the GDNF-Gel/HA-Mg nerve conduit in repairing peripheral nerve defects (Figure 1).

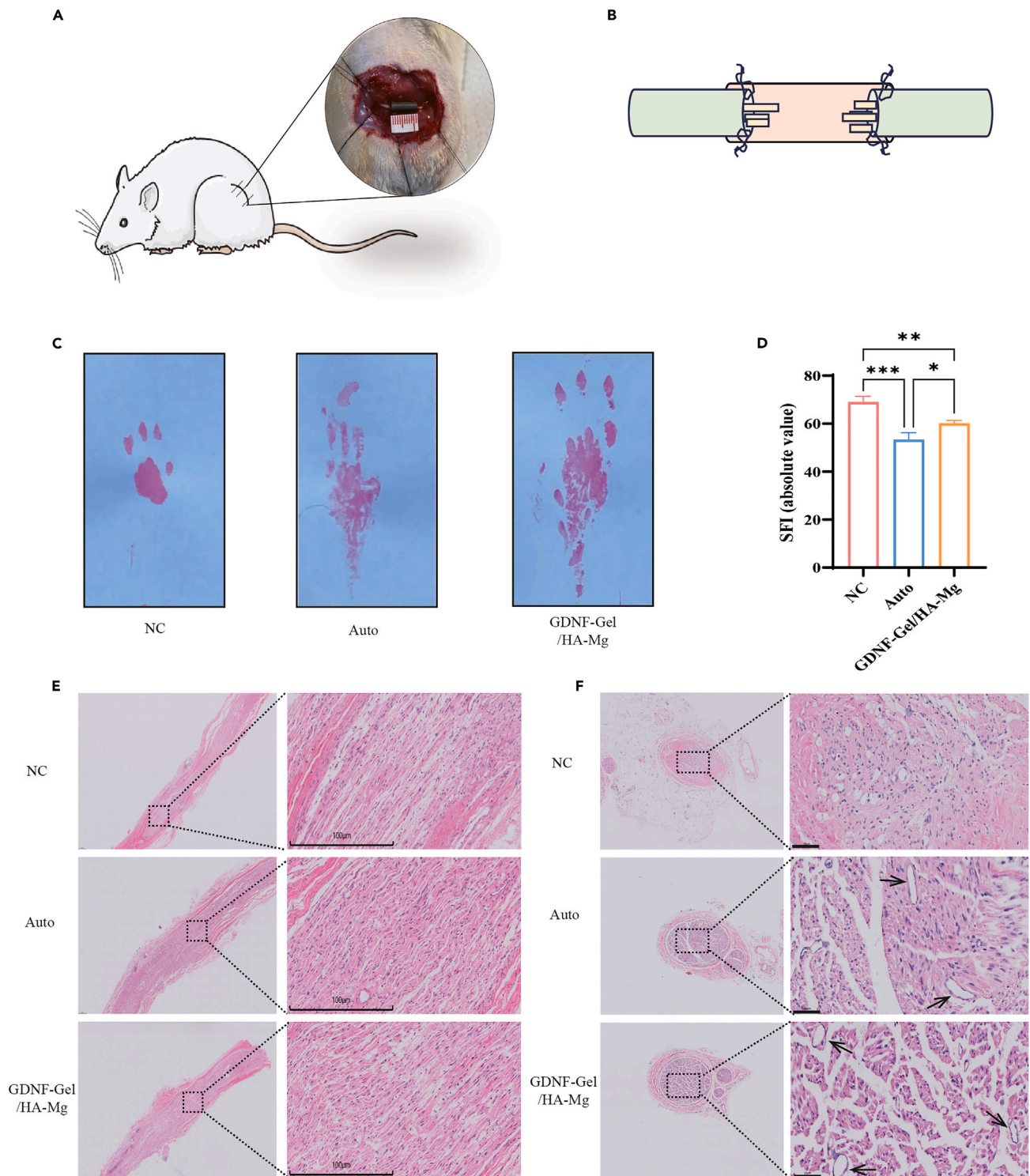


Figure 2. The effect of GDNF-Gel/HA-Mg conduit on sciatic functional index and never tissues regeneration

(A and B) diagram for implantation and suture of GDNF-Gel/HA-Mg conduit *in vivo*.

(C and D) the measurement of sciatic functional index and statistical analysis at 12 weeks post-surgery.

(E and F) Hematoxylin and Eosin (HE) staining of cross-sectional and longitudinal sections of regenerated nerves harvested at 12 weeks post-surgery. NC, negative control; Auto, autograft; GDNF, glial cell line-derived neurotrophic factor; GelMA, Gelatin methacryloyl; HA, hydroxylapatite; Mg, magnesium; SFI, sciatic functional index; ns, no statistical difference; * $p < 0.05$; ** $p < 0.01$; *** $p < 0.001$. scale bar: E:100 μ m; F: 50 μ m. Data are represented as mean \pm SEM.

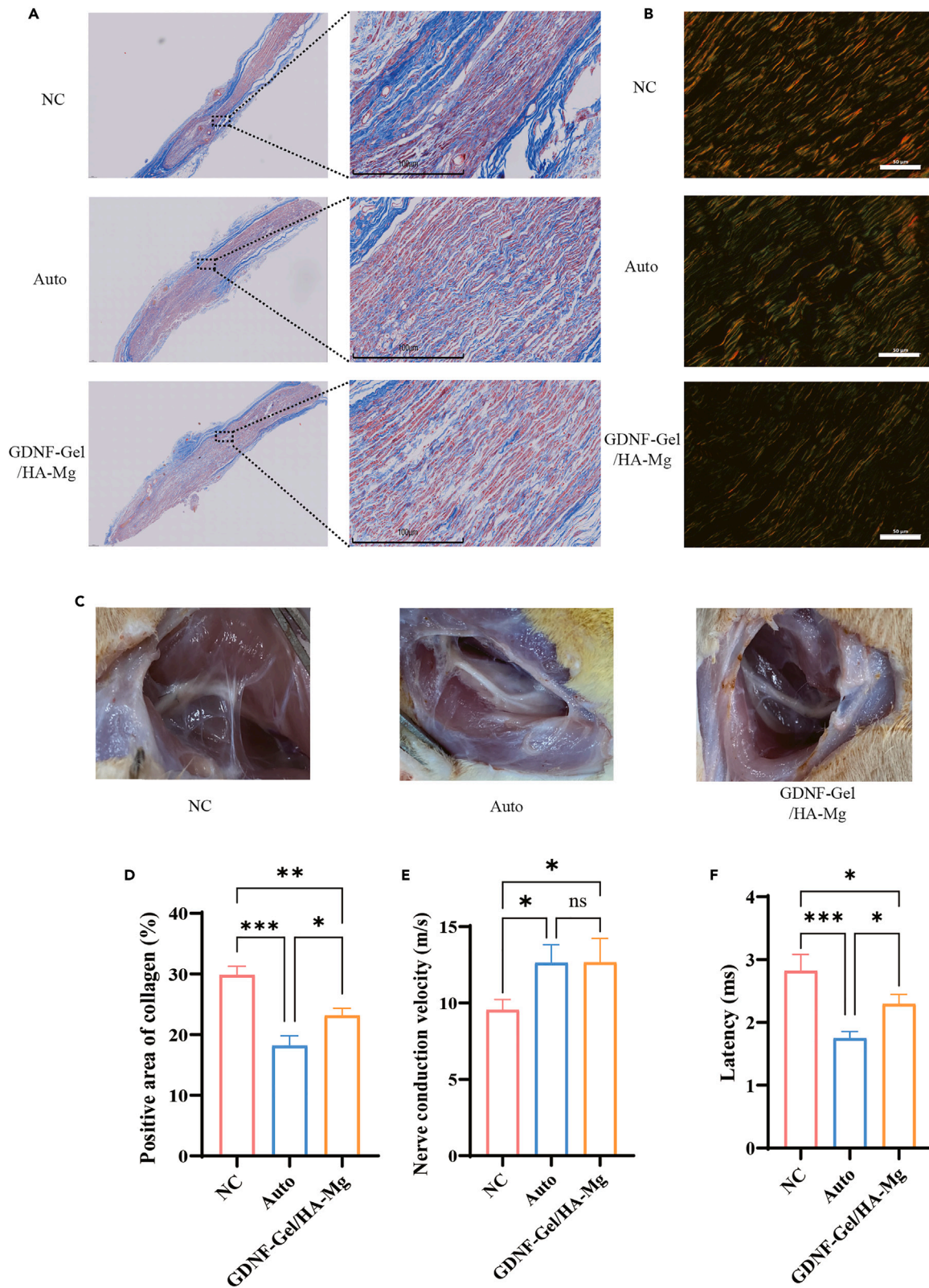


Figure 3. The effect of GDNF-Gel/HA-Mg conduit on never tissues regeneration and neuro-electrophysiology

(A and D) Masson Staining of regenerated nerves harvested at 12 weeks post-surgery and statistical analysis.

(B) Sirius Red Staining of regenerated nerves harvested at 12 weeks post-surgery.

(C) Assessment of the extent of adherence between regenerated nerves and adjacent tissues.

(E and F) The nerve conduction velocity and latency measurement of regenerated nerves at 12 weeks post-surgery. NC, negative control; Auto, autograft; GDNF, glial cell line-derived neurotrophic factor; GelMA, Gelatin methacryloyl; HA, hydroxylapatite; Mg, magnesium; ns, no statistical difference; * $p < 0.05$; ** $p < 0.01$; *** $p < 0.001$. scale bar: A:100 μm ; B: 50 μm . Data are represented as mean \pm SEM.

RESULTS**Preparation and characterization of GDNF-Gel/HA-Mg conduit**

The GDNF-Gel/HA-Mg conduit, designed for peripheral nerve defect repairment, was prepared by gradually coating the surface of Mg with HA and GDNF-Gel, as shown in [Figure 1](#). In order to systematically evaluate the corrosion resistance of GDNF-Gel/HA-Mg in PBS, corrosion resistance tests including electrochemical experiments, immersion tests, and hydrogen evolution tests were performed. The results showed that compared to Mg and HA-Mg, GDNF-Gel/HA-Mg exhibited the best corrosion resistance and could provide long-term protection to the magnesium substrate ([Figure S1](#)). Furthermore, the extract of GDNF-Gel/HA-Mg was obtained and co-cultured with Schwann cells, the results showed that the extract of GDNF-Gel/HA-Mg promoted the proliferation, migration, invasion of Schwann cells, and secretion of nerve growth factors ([Figures S2 and S3](#)).

GDNF-gel/HA-Mg nerve conduit promotes recovery of neural function

The GDNF-Gel/HA-Mg nerve conduit was sutured into a 10 mm defect model of rat sciatic nerve ([Figure 2A](#)). On both sides of the nerve conduit, there were two small circular holes with a diameter of approximately 1 mm. The conduit was firmly sutured to the sciatic nerve ends using 8-0 sutures passed through the small circular holes ([Figure 2B](#)), achieving secure fixation of the GDNF-Gel/HA-Mg nerve conduits *in vivo*. The untreated group with nerve defects was used as the negative control (NC group), and autologous nerve transplantation served as the positive control group (Auto group). The SFI of each group of rats was measured 12 weeks after surgery to evaluate neural function, and tissue samples were harvested for further experiments.

The results of sciatic functional index (SFI) measurement were shown in [Figures 2C and 2D](#), demonstrating that the recovery of sciatic nerve function in the GDNF-Gel/HA-Mg group was significantly superior to that of the NC group ($p < 0.01$), but was a little inferior to that of Auto group ($p < 0.05$).

GDNF-gel/HA-Mg nerve conduit promotes nerve fiber regeneration

Hematoxylin and Eosin (HE) staining revealed that in the NC group, the arrangement of nerve fibers was more disordered and sparse ([Figure 2E](#)), the cross-section revealed few and disorganized axon-like structures, lacking the organized pattern found in normal nerve tissue. Moreover, a substantial amount of connective tissue was present ([Figure 2F](#)). Conversely, both the Auto group and the GDNF-Gel/HA-Mg group exhibited parallel and wavy nerve fibers, densely and evenly distributed ([Figure 2E](#)). In the cross-section, regenerated axons were uniformly and orderly arranged, without the presence of disorganized fiber-filled tissue. Additionally, a greater number of newly formed blood vessels were observed ([Figure 2F](#)). Masson staining provided further evidence that the NC group had fewer regenerating nerve fiber tissues and an increased presence of collagen fiber deposits ([Figures 3A and 3D](#)). In contrast, the Auto group and the GDNF-Gel/HA-Mg group demonstrated a significant amount of newly formed nerve fiber tissue and fewer collagen fibers ([Figures 3A and 3D](#)).

In cases of peripheral nerve defects with long gaps, glial cells and fibroblasts tend to accumulate, leading to scar formation. This hinders the growth of nerve fiber and contributes to the development of neuromas, ultimately leading to poor outcomes in nerve repair. Sirius Red staining indicated a notable deposition of collagen fibers in the regenerative tissue of the NC group ([Figure 3B](#)). Macroscopically, adhesion between the regenerating nerve tissues and surrounding tissues was observed ([Figure 3C](#)). In the Auto group, there was reduced collagen fiber deposition, resulting in less adhesion between the regenerating nerve tissues and surrounding tissues ([Figures 3B and 3C](#)). Furthermore, the use of the GDNF-Gel/HA-Mg group further decreased collagen fiber deposition and minimized adhesion between the regenerating nerve tissues and surrounding tissues ([Figures 3B and 3C](#)).

GDNF-gel/HA-Mg nerve conduit enhances signal transmission and myelination of regenerating nerves, reducing atrophy in the peroneal muscles caused by denervation

Neurophysiological tests showed that both the Auto group and the GDNF-Gel/HA-Mg group had significantly better conduction velocity ([Figure 3E](#)) ($p < 0.05$) and shorter nerve potential latency compared to the NC group ([Figure 3F](#)). This suggests that GDNF-Gel/HA-Mg conduit treatment could effectively improve the signal transmission capacity of regenerated nerves.

Toluidine blue (TB) staining and transmission electron microscopy (TEM) were further used to investigate the formation of regenerating nerve axons and myelin. As depicted in [Figures 4A and 4C](#), the GDNF-Gel/HA-Mg group exhibited a larger number of regenerating nerve axons than the NC group ($p < 0.01$), while the Auto group had even more axons than the NC group ($p < 0.001$). Furthermore, TEM revealed that the NC group had significantly fewer nerve fibers, and exhibited severe demyelination, axonal atrophy, and poor fiber growth. In contrast, the Auto group and GDNF-Gel/HA-Mg group displayed clear nerve fiber structures, increasing fiber numbers, and marked improvement in

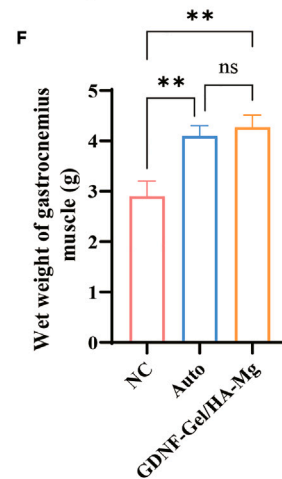
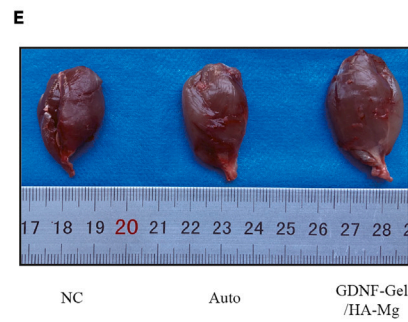
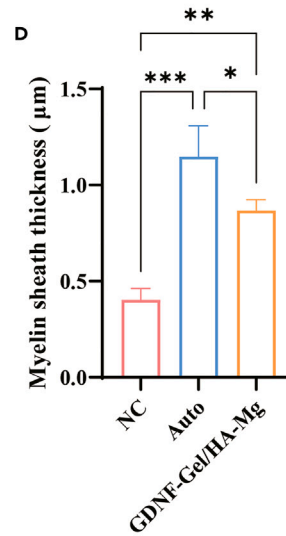
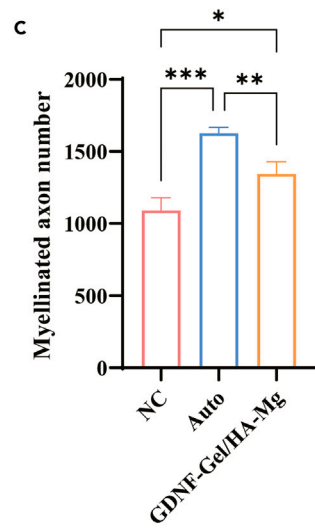
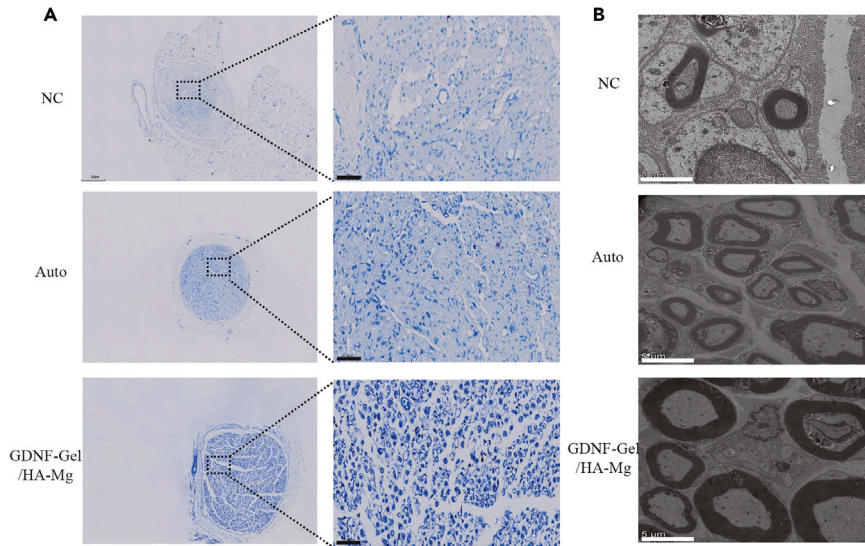


Figure 4. The effect of GDNF-Gel/HA-Mg conduit on regenerated axons and myelin

(A and C) Toluidine blue (TB) staining of regenerated nerves harvested at 12 weeks post-surgery and statistical analysis.

(B and D) myelin sheath thickness detected by transmission electron microscopy (TEM) and statistical analysis.

(E and F) Gastrocnemius muscle wet weight measurement and statistical analysis at 12 weeks post-surgery. NC, negative control; Auto, autograft; GDNF, glial cell line-derived neurotrophic factor; GelMA, Gelatin methacryloyl; HA, hydroxylapatite; Mg, magnesium; ns, no statistical difference; * $p < 0.05$; ** $p < 0.01$; *** $p < 0.001$. scale bar: A:50 μm ; B: 5 μm . Data are represented as mean \pm SEM.

demyelination (Figure 4B). Additionally, both the Auto group and GDNF-Gel/HA-Mg group showed greater average myelin sheath thickness in myelinated nerve fibers compared to the NC group (Figure 4D).

At 12 weeks post-surgery, the gastrocnemius muscles of each group were examined, morphology and size were compared. As shown in Figures 4E and 4F, the NC group exhibited pronounced muscle atrophy, whereas the Auto group and GDNF-Gel/HA-Mg group displayed milder atrophy (Figure 4F) ($p < 0.01$). These findings indicate that the GDNF-Gel/HA-Mg nerve conduit has a certain effect in alleviating muscle denervation atrophy after peripheral nerve defects.

GDNF-gel/HA-Mg nerve conduit enhances the expression of genes associated with nerve repair

S100 is commonly recognized as a specific marker for Schwann cells, and it plays a crucial role in their normal functioning, including the formation of Büngner bands, secretion of neurotrophic factors, and promotion of myelin formation. The level of S100 is indicative of the maturity of the nervous system function.¹⁹ Immunofluorescence (IF) results demonstrated a significant increase in S100 expression in both the Auto group and GDNF-Gel/HA-Mg group compared to the NC group ($p < 0.001$; Figures 5A and 5C). P75 is recognized as a marker of Schwann cells dedifferentiation, holds an important role in facilitating axonal growth and nerve regeneration.^{19,20} IF results indicated that GDNF-Gel/HA-Mg conduit treatment effectively elevated the expression of p75 in regenerating nerves ($p < 0.01$; Figures 5B and 5D), thereby contributing to nerve regeneration. Myelin basic protein (MBP) and neurofilament protein 200 (NF200) are pivotal in the process of myelin regeneration.²¹ We employed these two indicators to assess the impact of GDNF-Gel/HA-Mg on promoting axonal regeneration and the degree of myelination in regenerating nerves. The outcomes revealed a significant increase in the expression levels of NF200 and MBP in the GDNF-Gel/HA-Mg group compared to the NC group ($p < 0.001$; Figures 6A and 6B), with no notable difference observed when compared to the Auto group ($p > 0.05$).

GDNF-gel/HA-Mg nerve conduit promotes the repair of peripheral nerve defects by regulating PPAR- γ /RhoA/ROCK signaling pathway

The above experimental results provide evidence that the GDNF-Gel/HA-Mg nerve conduit effectively enhances the regeneration of peripheral nerves, making it an ideal substitute for autologous nerve transplantation in peripheral nerve defect repair. To gain further insight into the molecular mechanisms underlying the nerve repair properties of the GDNF-Gel/HA-Mg nerve conduit, nerve tissue samples from both the NC group and the GDNF-Gel/HA-Mg group were collected, RNA-seq and bioinformatics analysis were performed. The analysis results, including Principal Component Analysis (PCA) and clustering analysis, revealed significant differences in gene expression profiles between the two groups (Figures 7A and 7B). The differentially expressed genes based on a fold change ≥ 2 were selected, which showed that most gene expression levels tended to increase after treatment with GDNF-Gel/HA-Mg (Figures 7C and 7D). Notable differentially expressed genes included ENO3, Abs11, RBOX1, etc. (Figure 7E). GO enrichment analysis indicated that these differentially expressed genes were primarily associated with cellular components such as the membrane, cell periphery, contractile fibers, extracellular space, etc. (Figure 7F). Furthermore, KEGG pathway enrichment analysis demonstrated that these differentially expressed genes were mainly enriched in signaling pathways such as allograft rejection, peroxisome proliferator-activated receptor (PPAR) signaling pathway, cell adhesion molecules, etc. (Figure 7G). Moreover, Gene Set Enrichment Analysis (GSEA) enrichment analysis revealed a significant upregulation of the PPAR signaling pathway following treatment with the GDNF-Gel/HA-Mg nerve conduit (Figure 7H). Based on these bioinformatics analysis findings, regenerated nerve tissue samples from both the NG group and the GDNF-Gel/HA-Mg group were obtained to validate the results using IF, quantitative real-time PCR (qPCR) and Western blotting. The IF and qPCR results exhibited a significant increase in the expression of PPAR- γ in the GDNF-Gel/HA-Mg group compared to the NC group (Figures 8A–8C). Additionally, qPCR and Western blotting revealed that the downstream RhoA/Rho-associated kinase (ROCK) signaling pathway of PPAR- γ was inhibited in the GDNF-Gel/HA-Mg group (Figures 8D–8I). Taken together, these findings suggest that the GDNF-Gel/HA-Mg nerve conduit promotes the regeneration of peripheral nerves by regulating PPAR- γ /RhoA/ROCK signaling pathway.

Biological safety assessment of GDNF-Gel/HA-Mg conduit

To further evaluate the biological safety of the GDNF-Gel/HA-Mg conduit in SD rats, the functions and pathological structures of major organs such as the heart, liver, spleen, lung, and kidney were examined. The results indicated that there were no significant differences in creatine kinase (CK), creatine kinase isoenzyme-MB (CK-MB), and lactic dehydrogenase (LDH) levels among all groups (Figure 9A). Additionally, no noticeable changes in myocardial structure were observed after implantation of the GDNF-Gel/HA-Mg conduit (Figure 9B), suggesting that the conduit did not have a toxic effect on the heart. Similarly, the levels of alanine aminotransferase (ALT), aspartate aminotransferase (AST) and creatinine (Figure 9A), as well as the histological examination results of the liver, spleen, lung, and kidney (Figures 9C–9F), all indicated that the GDNF-Gel/HA-Mg conduits have good biological safety and may be a potential candidate for repairing peripheral nerve defects.

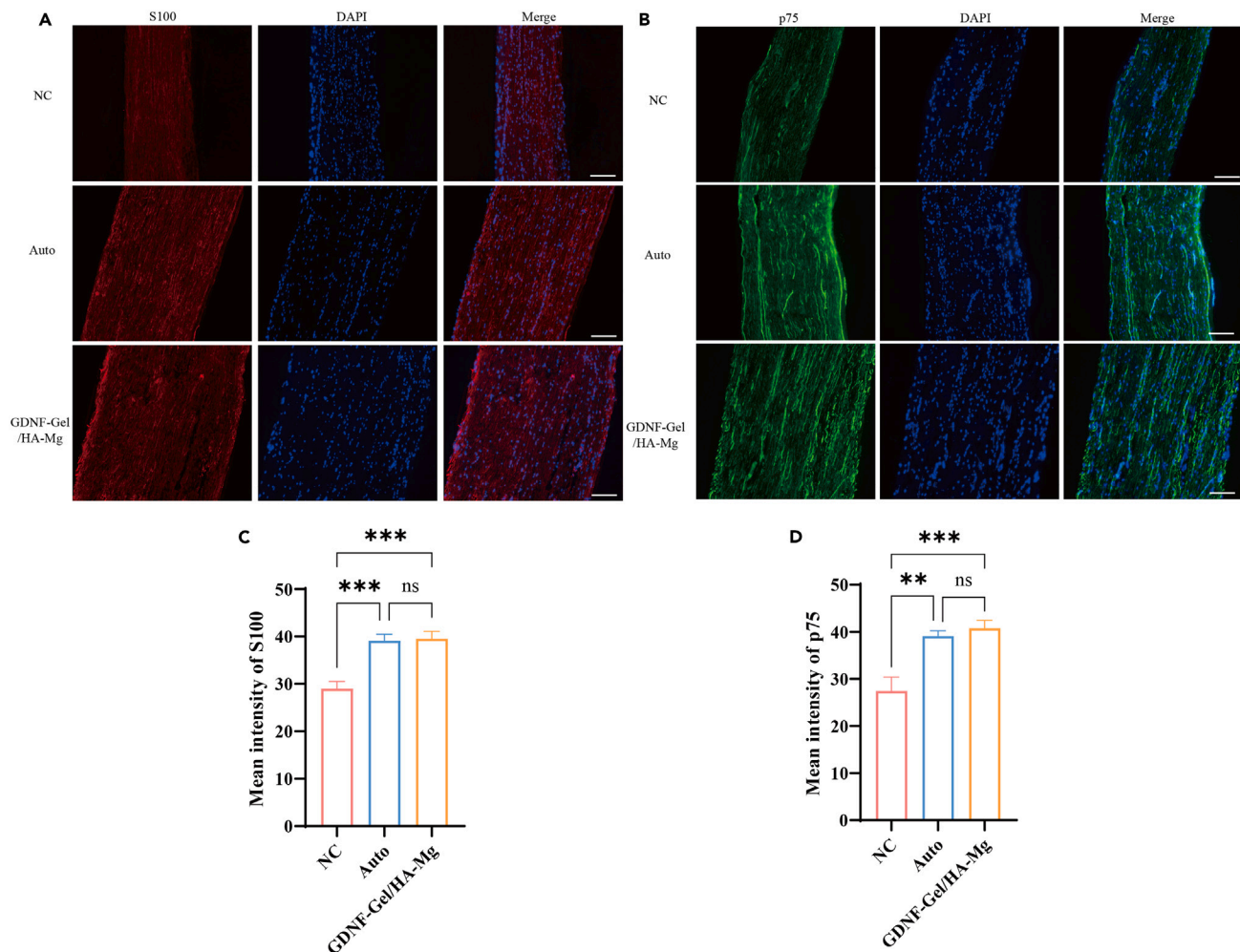


Figure 5. The expression of S100 and p75 at 12 weeks post-surgery

(A and C) The expression of S100 detected by immunofluorescence and statistical analysis.

(B and D) The expression of p75 detected by immunofluorescence and statistical analysis. NC, negative control; Auto, autograft; GDNF, glial cell line-derived neurotrophic factor; GelMA, Gelatin methacryloyl; HA, hydroxylapatite; Mg, magnesium; SFI, sciatic functional index; ns, no statistical difference; ** $p < 0.01$; *** $p < 0.001$. scale bar: 50 μ m. Data are represented as mean \pm SEM.

DISCUSSION

Magnesium, as an essential element in the human body, plays a crucial role in maintaining normal nervous system function. Previous studies have shown that Mg^{2+} could alleviate secondary injury after primary PNI by regulating cell function, antagonizing N-methyl-D-aspartate receptors (NMDA receptors), and inhibiting calcium influx, thus providing protection to peripheral nerves.^{13,14} In recent years,^{5,13} the role of magnesium in the repair of peripheral nerve injuries has gained considerable attention,²² and more and more Mg-based nerve conduits are being used for PNI repairment. Li B.H. et al.²³ bridged the two ends of acute sciatic nerve injury using Mg wire and found that the use of Mg wire effectively promotes the recovery of sciatic nerve function and facilitates the expression of nerve growth factor and its receptor p75, thereby effectively promoting the repair of peripheral nerve injuries.

However, there are still limitations in the current application of Mg-base conduits for repairing peripheral nerve defects. One major issue is the rapid degradation rate of Mg, which prevents it from providing continuous mechanical support and guidance throughout the process of peripheral nerve repair.¹³ Additionally, its corrosion resistance is poor, and a large amount of hydrogen could be generated during rapid degradation, which could affect the pH value of the local neural growth microenvironment, thereby interfering with nerve regeneration.¹³

To address these challenges, researchers have been increasingly exploring various Mg-based metallic materials, including magnesium alloys, for PNI repair. For instance, Fei et al.²⁴ investigated the potential of three magnesium alloys: NZ20 (Mg-Sn-Zn), ZN20 (Mg-2Zn-Nd), and Mg-10Li. Their study revealed that these alloys exhibited slightly prolonged degradation rates compared to Mg. However, NZ20 demonstrated cytotoxicity. It's important to note that the *in vitro* experiments utilized endothelial cells instead of the specific cells involved in the process of PNI repair, such as Schwann cells. Another study by Almansoori et al.²⁵ focused on PNI repair using hydroxyapatite-coated WE43 (HA-WE43). The

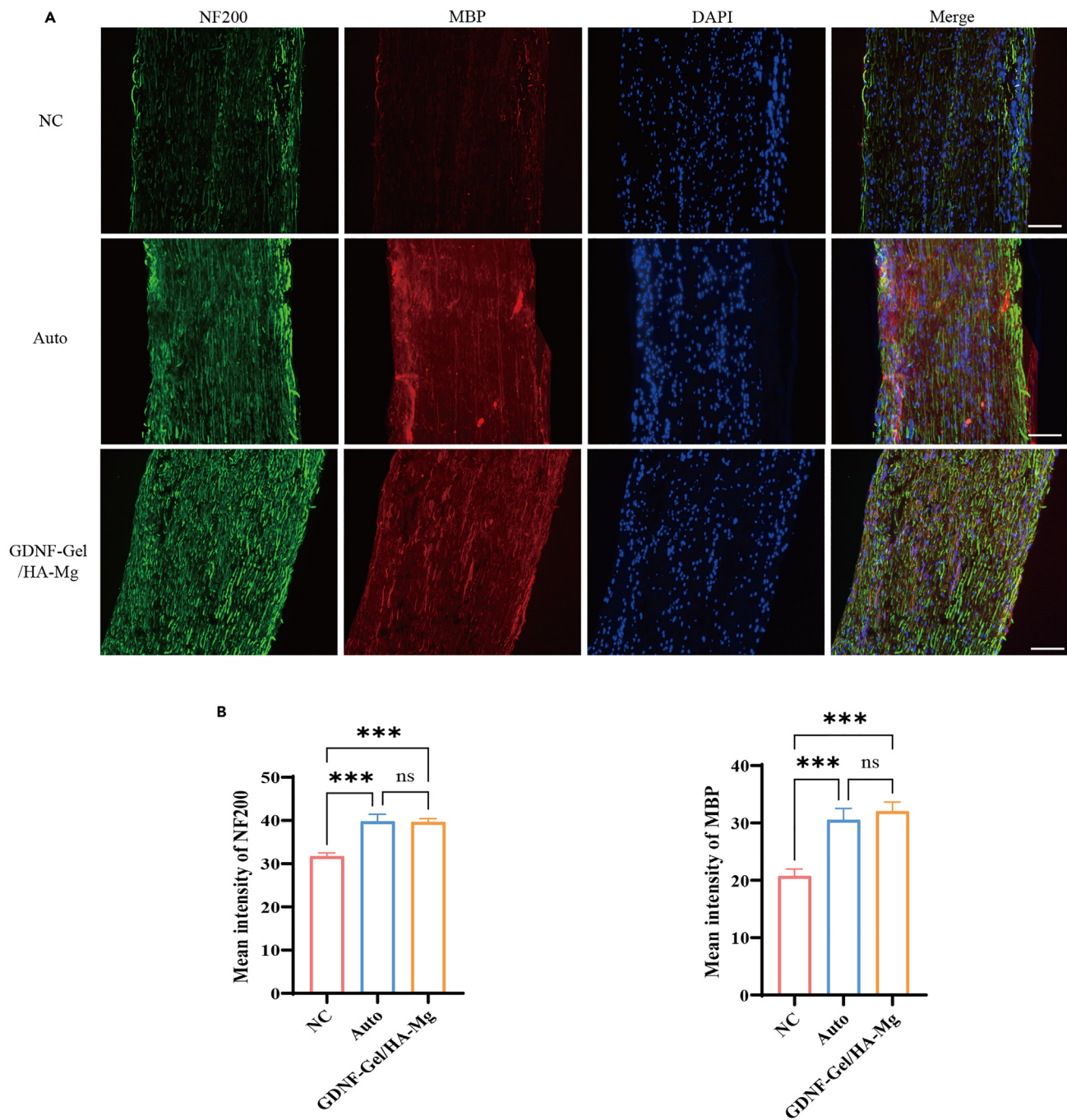


Figure 6. The expression of neurofilament-200 (NF-200) and myelin basic protein (MBP) at 12 weeks post-surgery

(A) The expression of neurofilament-200 (NF-200) and myelin basic protein (MBP) detected by immunofluorescence.

(B) statistical analysis. NF-200, neurofilament-200; MBP, myelin basic protein; NC, negative control; Auto, autograft; GDNF, glial cell line-derived neurotrophic factor; GelMA, Gelatin methacryloyl; HA, hydroxylapatite; Mg, magnesium; SFI, sciatic functional index; ns, no statistical difference; *** $p < 0.001$. scale bar: 50 μ m. Data are represented as mean \pm SEM.

researchers found that HA-WE43 promoted the adhesion and proliferation of pheochromocytoma cells (PC12), but it didn't have a significant effect on Schwann cells. Although *in vivo* experiments indicated that HA-WE43 could prolong the degradation time of magnesium and reduce hydrogen production during degradation, its ability to promote sciatic nerve repair was limited. Therefore, improving the corrosion resistance of Mg-base conduit, delaying its degradation time, and enhancing its bioactivity are key factors for further promoting its application.

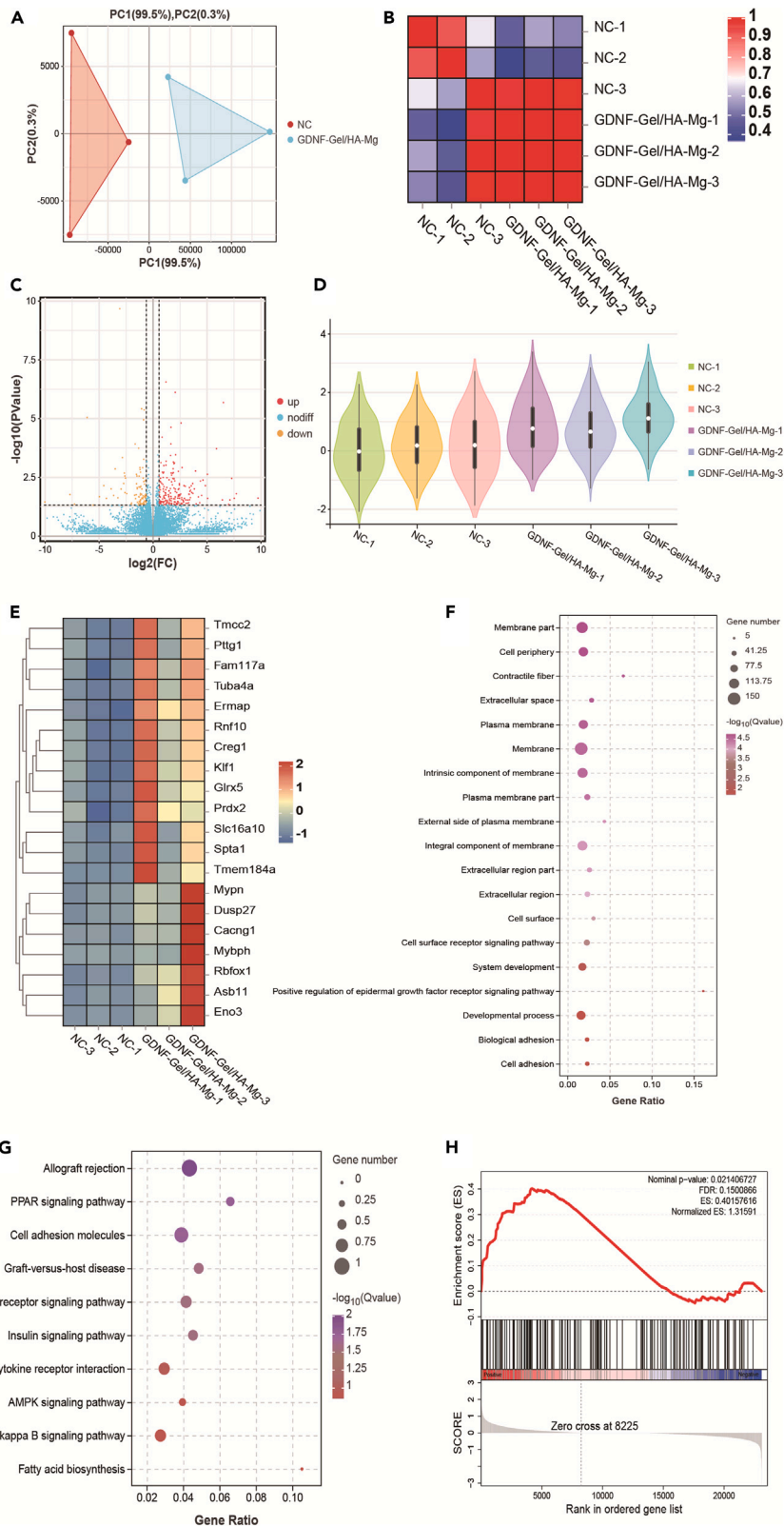


Figure 7. The bioinformatics analysis results

- (A and B) Principal Component Analysis (PCA) and Cluster analysis of samples.
(C) Volcano map of differentially expressed genes.
(D) The mRNA expression level of differentially expressed gene.
(E) Cluster analysis of differentially expressed genes.
(F) GO Enrichment Analysis of differentially expressed genes.
(G) KEGG Pathway Enrichment Analysis of differentially expressed genes.
(H) Gene Set Enrichment Analysis (GSEA) of PPAR signaling pathway between NC and GDNF-Gel/HA-Mg group; NC, negative control; GDNF, glial cell line-derived neurotrophic factor; GelMA, Gelatin methacryloyl; HA, hydroxylapatite; Mg, magnesium; FC, fold change.

In this study, we initially modified Mg with an HA coating using liquid-phase deposition, resulting in HA-Mg. GelMA hydrogel is a biocompatible biomaterial known for its excellent biocompatibility and sustained release properties, making it widely used for cytokine delivery.^{26,27} In order to further enhance the bioactivity of HA-Mg, we loaded GelMA hydrogel with GDNF and combined it with HA-Mg through photopolymerization, yielding GDNF-Gel/HA-Mg nerve conduits. Compared to Mg, GDNF-Gel/HA-Mg exhibited significantly improved corrosion resistance. *In vivo* experiments demonstrated that GDNF-Gel/HA-Mg nerve conduits effectively promoted nerve fiber regeneration as well as functional recovery of the sciatic nerve. They also significantly facilitated axonal regeneration and remyelination of regenerating nerves. Furthermore, GDNF-Gel/HA-Mg nerve conduits effectively promoted the expression of nerve regeneration-related genes, thereby facilitating the process of peripheral nerve repair. Importantly, GDNF-Gel/HA-Mg nerve conduits played a significant role in promoting axonal regeneration and alleviating denervation atrophy in the gastrocnemius muscle. Therefore, GDNF-Gel/HA-Mg nerve conduit is an ideal candidate for nerve defect repair, offering potential as alternatives to autografts and providing new avenues and strategies for the repairment of peripheral nerve defects.

In this study, we further investigated the potential molecular mechanisms underlying the promotion of peripheral nerve defect repair by GDNF-Gel/HA-Mg nerve conduits. The results indicate that GDNF-Gel/HA-Mg conduits might promote peripheral nerve defects repair by activating PPAR- γ and inhibiting the RhoA/ROCK signaling pathway. Rho family proteins, including RhoA, Cdc42, and Rac, are a group of guanosine triphosphate (GTP)-binding proteins that regulate various cellular processes, also known as Rho-GTPases due to their GTPase activity.²⁸ It is widely recognized that RhoA plays a significant role in growth cone collapse and axonal retraction, thus serving as a negative regulator of neurite formation and maintenance.^{28,29} ROCK, as an effector of Rho-GTPases, plays an important role in regulating neuronal cell cytoskeleton. Activation of the Rho/ROCK signaling pathway following nerve injury inhibits axonal growth and promotes growth cone collapse, impairing nerve regeneration and functional recovery.^{28–30} Consequently, the targeting of the Rho/ROCK signaling pathway serves as an effective strategy for enhancing PNI repairment.

PPAR- γ is a type of nuclear receptor belonging to the transcription factor family, involved in the regulation of gene transcription and expression. It plays an important role in physiological processes such as lipid metabolism, inflammatory response, cell proliferation, and differentiation.³¹ Researches have shown that PPAR- γ could inhibit RhoA/ROCK activation by converting inactive guanosine diphosphate (GDP)-Rho to active guanosine triphosphate (GTP)-Rho.^{32,33} Therefore, an increasing number of PPAR- γ agonists or drugs have been developed and utilized for the repair of PNI.³⁴ The present work found that GDNF-Gel/HA-Mg conduits treatment could activate PPAR- γ in peripheral nerve tissue, thereby inhibiting the activation of the RhoA/ROCK signaling pathway and effectively promoting peripheral nerve defect repair. Previous studies have demonstrated that supplementation with Mg could effectively increase the expression of PPAR- γ .^{35,36} Therefore, in this study, the regulation of the PPAR- γ /RhoA/ROCK signaling pathway by GDNF-Gel/HA-Mg conduits to promote nerve regeneration processes is likely mainly achieved through the release of Mg²⁺.

Yao et al.⁵ have showed that Mg²⁺ could promote the growth of neuronal axons in a concentration-dependent manner through the activation of the PI3K/Akt signaling pathway and Sema5b, which is inconsistent with the present work to some extent, the reasons might be attributed to followings: first, they have used a magnesium-encapsulated injectable hydrogel and 3D-engineered polycaprolactone conduit, which is largely different from conduit used in this study, thus, the molecular mechanisms involved might be totally different, the regenerated nerve tissues from NC group and GDNF-Gel/HA-Mg group were collected in this study for RNA-seq and bioinformatics analysis, based on these results, we have screened some highly related pathways and further verification experiments were performed, and showed that GDNF-Gel/HA-Mg might be involved in the repair of peripheral nerve defects by regulating the PPAR- γ /RhoA/ROCK signaling pathway; second, in study performed by Yao et al.,⁵ they have isolated dorsal root ganglia (DRG) neurons for *in vitro* study, then the DRG neurons were treated with varying Mg²⁺ concentrations (Ctrl, 10, 20, 30, 40, and 50 mM), after that, these neurons were collected for RNA-seq and qPCR, and concluded that Mg²⁺ could promote neurite outgrowth via the PI3K-AKT signaling pathway and Sema5b. However, in the present work, the regenerated nerve tissues were collected for RNA-seq and bioinformatics analysis, the results showed that the PPAR signaling pathway is most likely the key pathway mediating the promotion of neural repair by GDNF-G/HA-Mg, since different samples in Yao et al.⁵ and the present work were used, the molecular mechanisms involved might be also different.

In summary, we have developed a Mg-based nerve conduit known as GDNF-Gel/HA-Mg nerve conduit that provides sustained release of nerve growth factors. This innovative conduit effectively enhanced nerve regeneration and promoted functional recovery. It also has the potential to alleviate denervation atrophy of the gastrocnemius muscle and facilitate axonal regrowth and myelination after PNI. The GDNF-Gel/HA-Mg conduit achieves these outcomes primarily by modulating the PPAR- γ /RhoA/ROCK signaling pathway. Consequently, this strategy holds great promise as a viable alternative to autologous nerves for repairing peripheral nerve defects.

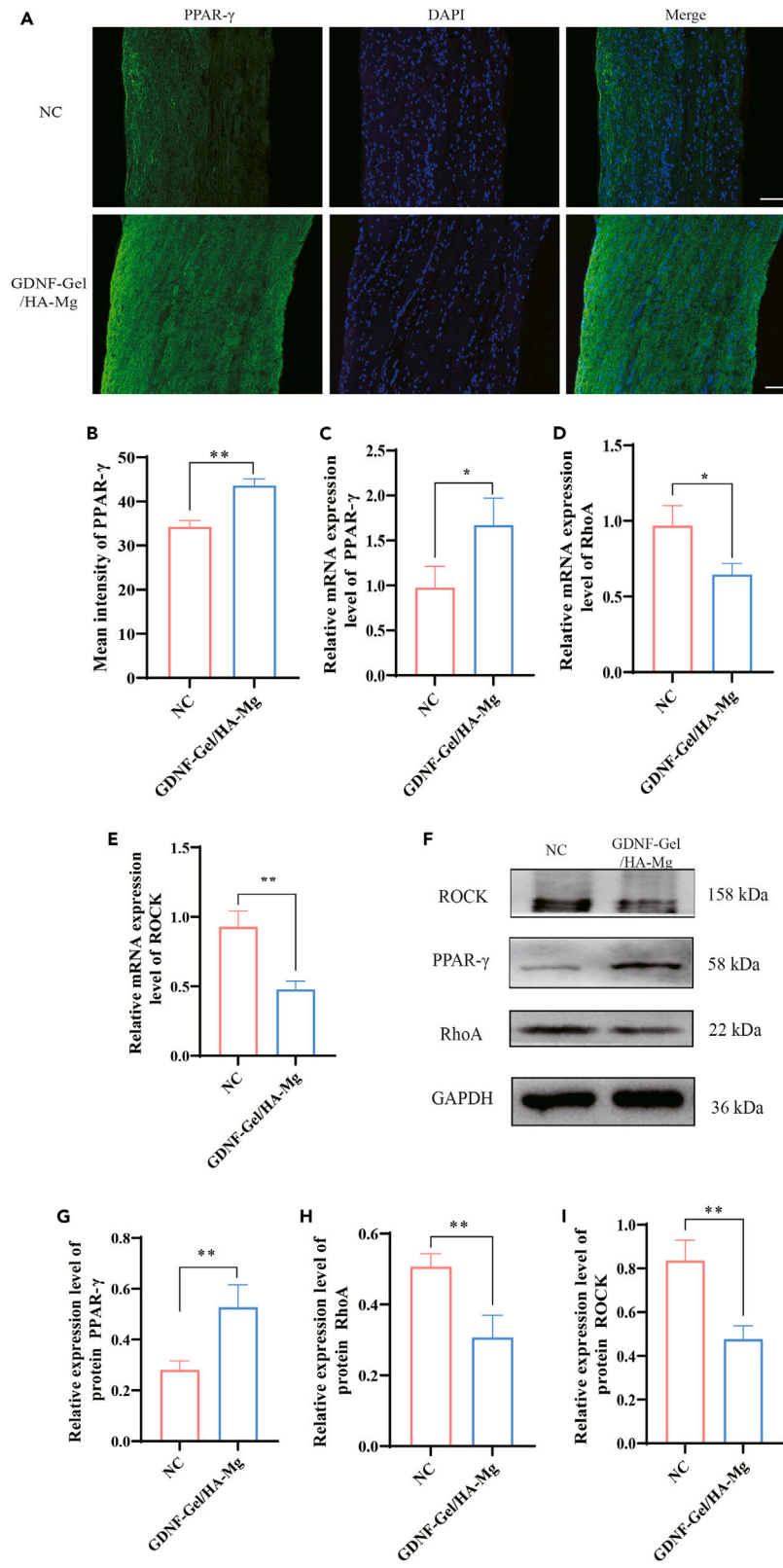


Figure 8. The expression levels of PPAR- γ /RhoA/ROCK signaling pathway

(A and B) The expression of PPAR- γ detected by immunofluorescence and statistical analysis; (C–E) the relative mRNA expression level of PPAR- γ , Rho, ROCK and statistical analysis; (F–I) The expression of peroxisome proliferator-activated receptor gamma (PPAR- γ), RhoA, Rho-associated kinase (ROCK) by western blotting and statistical analysis. NC: negative control; GDNF: glial cell line-derived neurotrophic factor; GelMA: Gelatin methacryloyl; HA: hydroxylapatite; Mg: magnesium; PPAR- γ : peroxisome proliferator-activated receptor gamma; ROCK: Rho-associated kinase; * $p < 0.05$; ** $p < 0.01$. scale bar: 50 μ m. Data are represented as mean \pm SEM.

Limitations of the study

There are still limitations to this research: (1) The study did not fully elucidate the role of GDNF-Gel/HA-Mg conduits in repairing long-gap nerve defects. Future studies should focus on designing longer GDNF-Gel/HA-Mg conduits and constructing long-gap nerve defect models in dogs or monkeys, then GDNF-Gel/HA-Mg nerve conduits should be implanted *in vivo* to explore their value in repairing long-distance nerve defects. (2) The GDNF-Gel/HA-Mg nerve conduits developed in this study only contained GDNF and did not accurately replicate the microenvironment required for nerve growth. Subsequent studies should consider incorporating other essential neurotrophic factors to create a favorable microenvironment for nerve growth by controlling the release of different factors at different regeneration stages.

STAR★METHODS

Detailed methods are provided in the online version of this paper and include the following:

- KEY RESOURCES TABLE
- RESOURCE AVAILABILITY
 - Lead contact
 - Materials availability
 - Data and code availability
- EXPERIMENTAL MODEL AND STUDY PARTICIPANT DETAILS
 - Rat
- METHOD DETAILS
 - Preparation and characterization of GDNF-Gel/HA-Mg nerve conduit
 - The sciatic nerve defect model in SD rats and implantation of GDNF-Gel/HA-Mg nerve conduit
 - Measurement of sciatic functional index (SFI)
 - Hematoxylin and eosin (HE) staining
 - Masson staining, sirius red staining
 - Myelinated nerve fibers and myelin sheath thickness measurement
 - Neurophysiology and gastrocnemius muscle wet weight measurement
 - Immunofluorescence (IF)
 - Quantitative real-time PCR (qPCR)
 - Western blotting
 - RNA-seq and bioinformatics analysis
 - Biological safety assessment
- QUANTIFICATION AND STATISTICAL ANALYSIS

SUPPLEMENTAL INFORMATION

Supplemental information can be found online at <https://doi.org/10.1016/j.isci.2024.108969>.

ACKNOWLEDGMENTS

The present work was supported by National Natural Science Foundation of China (82171370); Key Research and Development Program of the Shaanxi Province (2019SF-113; 2022SF-192); Foreign Cooperation Project of Science and Technology, Fujian Province (2021I0012).

AUTHOR CONTRIBUTIONS

Study conceptualization: W.Y., D.X.Q., and F.X.Y.; study implementation: C.Y.Q. and C.Y.; data collection: L.Y., Z.G.Y., and Z.J.N.; manuscript writing: C.Y.Q. and C.Y.; manuscript review and editing: L.Y. and L.L.F.; study supervision: Z.G.Y. and L.L.F.. All authors approved the final version of the manuscript.

DECLARATION OF INTERESTS

The authors declare that they have no competing interests.

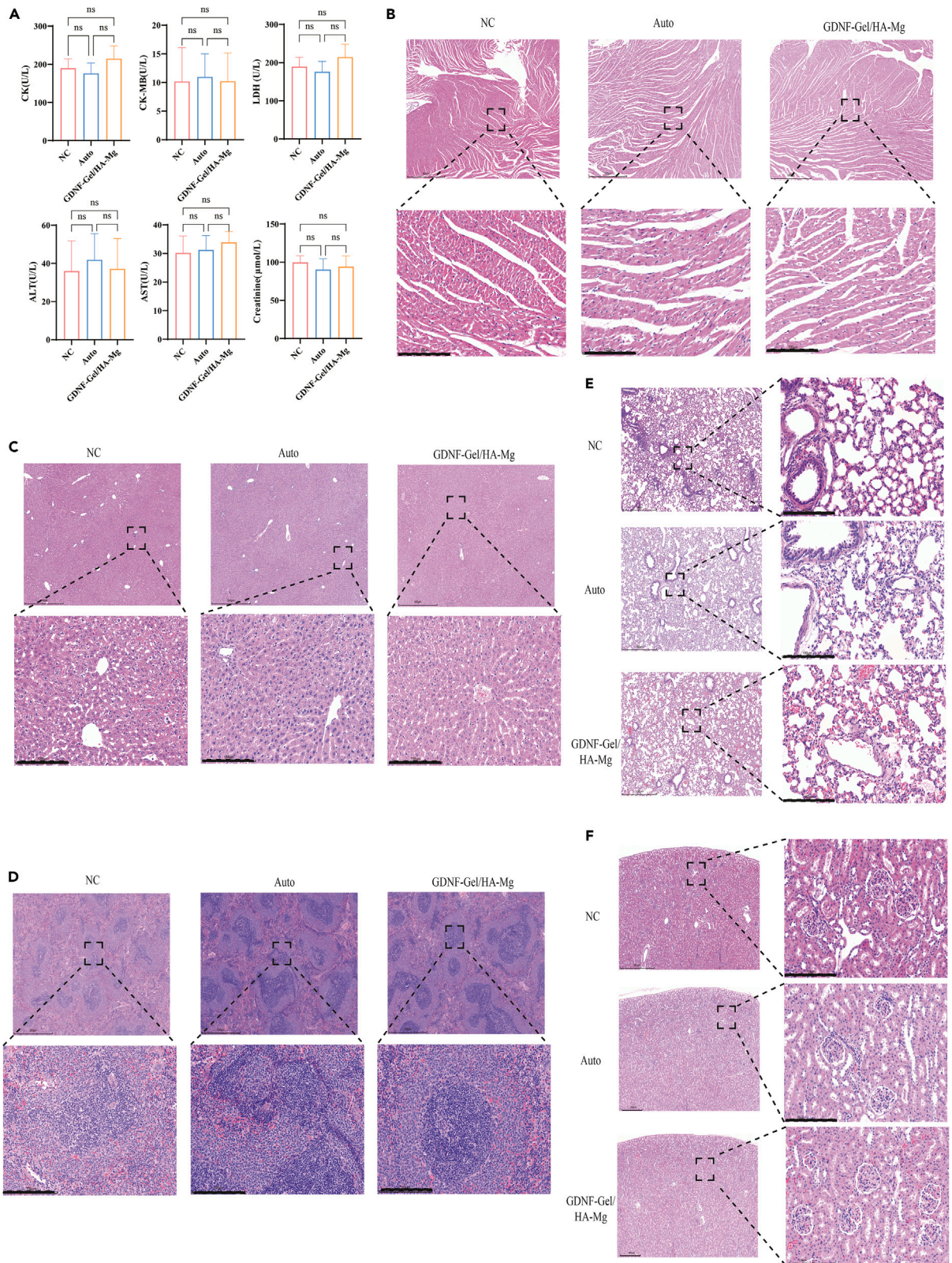


Figure 9. Biological safety assessment of GDNF-Gel/HA-Mg in vivo

(A) The levels of myocardial enzymes, transaminases, and renal function and quantitative analysis. (B–F) HE results of heart (B), liver(C), spleen(D), lung(E) and kidney(F) from different groups. CK, creatine kinase; CK-MB, creatine kinase isoenzyme-MB; LDH, lactic dehydrogenase; ALT, alanine aminotransferase; AST, aspartate aminotransferase; NC, negative control; GDNF, glial cell line-derived neurotrophic factor; GelMA, Gelatin methacryloyl; HA, hydroxylapatite; Mg, magnesium; ns, no statistical difference. Scale bar: 100µm. Data are represented as mean ± SEM.

Received: August 28, 2023
Revised: November 16, 2023
Accepted: January 16, 2024
Published: January 19, 2024

REFERENCES

- Modrak, M., Talukder, M.A.H., Gurgenschvili, K., Noble, M., and Elfar, J.C. (2020). Peripheral nerve injury and myelination: Potential therapeutic strategies. *J. Neurosci. Res.* 98, 780–795. <https://doi.org/10.1002/jnr.24538>.
- Wang, M.L., Rivlin, M., Graham, J.G., and Beredjikian, P.K. (2019). Peripheral nerve injury, scarring, and recovery. *Connect. Tissue Res.* 60, 3–9. <https://doi.org/10.1080/03008207.2018.1489381>.
- Battiston, B., Titolo, P., Ciclamini, D., and Panero, B. (2017). Peripheral Nerve Defects: Overviews of Practice in Europe. *Hand Clin.* 33, 545–550. <https://doi.org/10.1016/j.hcl.2017.04.005>.
- Vijayavenkataraman, S. (2020). Nerve guide conduits for peripheral nerve injury repair: A review on design, materials and fabrication methods. *Acta Biomater.* 106, 54–69. <https://doi.org/10.1016/j.actbio.2020.02.003>.
- Yao, Z., Yuan, W., Xu, J., Tong, W., Mi, J., Ho, P.-C., Chow, D.H.K., Li, Y., Yao, H., Li, X., et al. (2022). Magnesium-Encapsulated Injectable Hydrogel and 3D-Engineered Polycaprolactone Conduit Facilitate Peripheral Nerve Regeneration. *Adv. Sci.* 9, e2202102. <https://doi.org/10.1002/adv.202202102>.
- Pabari, A., Lloyd-Hughes, H., Seifalian, A.M., and Mosahebi, A. (2014). Nerve conduits for peripheral nerve surgery. *Plast. Reconstr. Surg.* 133, 1420–1430. <https://doi.org/10.1097/PRS.0000000000000226>.
- Song, S., Wang, X., Wang, T., Yu, Q., Hou, Z., Zhu, Z., and Li, R. (2020). Additive Manufacturing of Nerve Guidance Conduits for Regeneration of Injured Peripheral Nerves. *Front. Bioeng. Biotechnol.* 8, 590596. <https://doi.org/10.3389/fbioe.2020.590596>.
- Konofaos, P., and Ver Halen, J.P. (2013). Nerve repair by means of tubulization: past, present, future. *J. Reconstr. Microsurg.* 29, 149–164. <https://doi.org/10.1055/s-0032-1333316>.
- Chang, W., Shah, M.B., Lee, P., and Yu, X. (2018). Tissue-engineered spiral nerve guidance conduit for peripheral nerve regeneration. *Acta Biomater.* 73, 302–311. <https://doi.org/10.1016/j.actbio.2018.04.046>.
- Geuna, S., Tos, P., Battiston, B., and Giacobini-Robecchi, M.G. (2004). Bridging peripheral nerve defects with muscle-vein combined guides. *Neurol. Res.* 26, 139–144. <https://doi.org/10.1179/016164104225013752>.
- Lu, Q., Zhang, F., Cheng, W., Gao, X., Ding, Z., Zhang, X., Lu, Q., and Kaplan, D.L. (2021). Nerve Guidance Conduits with Hierarchical Anisotropic Architecture for Peripheral Nerve Regeneration. *Adv. Healthc. Mater.* 10, e2100427. <https://doi.org/10.1002/adhm.202100427>.
- Long, Q., Wu, B., Yang, Y., Wang, S., Shen, Y., Bao, Q., and Xu, F. (2021). Nerve guidance conduit promoted peripheral nerve regeneration in rats. *Artif. Organs* 45, 616–624. <https://doi.org/10.1111/aor.13881>.
- Zhang, J., Zhang, B., Zhang, J., Lin, W., and Zhang, S. (2021). Magnesium Promotes the Regeneration of the Peripheral Nerve. *Front. Cell Dev. Biol.* 9, 717854. <https://doi.org/10.3389/fcell.2021.717854>.
- de Baaij, J.H.F., Hoenderop, J.G.J., and Bindels, R.J.M. (2015). Magnesium in man: implications for health and disease. *Physiol. Rev.* 95, 1–46. <https://doi.org/10.1152/physrev.00012.2014>.
- Pan, H.-C., Sheu, M.-L., Su, H.-L., Chen, Y.-J., Chen, C.-J., Yang, D.-Y., Chiu, W.-T., and Cheng, F.-C. (2011). Magnesium supplement promotes sciatic nerve regeneration and down-regulates inflammatory response. *Magnes. Res.* 24, 54–70. <https://doi.org/10.1684/mrh.2011.0280>.
- May, F., Buchner, A., Matiassek, K., Schlenker, B., Stief, C., and Weidner, N. (2016). Recovery of erectile function comparing autologous nerve grafts, unseeded conduits, Schwann-cell-seeded guidance tubes and GDNF-overexpressing Schwann cell grafts. *Dis. Model. Mech.* 9, 1507–1511. <https://doi.org/10.1242/dmm.026518>.
- Ee, X., Yan, Y., Hunter, D.A., Schellhardt, L., Sakiyama-Elbert, S.E., Mackinnon, S.E., and Wood, M.D. (2017). Transgenic SCs expressing GDNF-IRES-DsRed impair nerve regeneration within acellular nerve allografts. *Biotechnol. Bioeng.* 114, 2121–2130. <https://doi.org/10.1002/bit.26335>.
- Zhang, L., Ma, Z., Smith, G.M., Wen, X., Pressman, Y., Wood, P.M., and Xu, X.-M. (2009). GDNF-enhanced axonal regeneration and myelination following spinal cord injury is mediated by primary effects on neurons. *Glia* 57, 1178–1191. <https://doi.org/10.1002/glia.20840>.
- Ebenezer, G.J., Pena, M.T., Daniel, A.S., Truman, R.W., Adams, L., Duthie, M.S., Wagner, K., Zampino, S., Tolf, E., Tsottles, D., and Polydefkis, M. (2022). Mycobacterium leprae induces Schwann cell proliferation and migration in a denervated milieu following intracutaneous excision axotomy in nine-banded armadillos. *Exp. Neurol.* 352, 114053. <https://doi.org/10.1016/j.expneurol.2022.114053>.
- Fang, X., Zhang, C., Zhang, C., Cai, Y., Yu, Z., Huang, Z., Li, W., and Zhang, W. (2019). Reactivation of Denervated Schwann Cells by Embryonic Spinal Cord Neurons to Promote Axon Regeneration and Remyelination. *Stem Cells Int.* 2019, 7378594. <https://doi.org/10.1155/2019/7378594>.
- Yongguang, L., Xiaowei, W., Huichao, Y., and Yanxiang, Z. (2022). Gastrodin promotes the regeneration of peripheral nerves by regulating miR-497/BDNF axis. *BMC Complement. Med. Ther.* 22, 45. <https://doi.org/10.1186/s12906-021-03483-z>.
- Wang, N., Yang, S., Shi, H., Song, Y., Sun, H., Wang, Q., Tan, L., and Guo, S. (2022). Magnesium alloys for orthopedic applications: A review on the mechanisms driving bone healing. *J. Magnes. Alloy.* 10, 3327–3353. <https://doi.org/10.1016/j.jma.2022.11.014>.
- Li, B.-H., Yang, K., and Wang, X. (2016). Biodegradable magnesium wire promotes regeneration of compressed sciatic nerves. *Neural Regen. Res.* 11, 2012–2017. <https://doi.org/10.4103/1673-5374.197146>.
- Fei, J., Wen, X., Lin, X., Sajilafu Wang, W., Wang, W., Ren, O., Chen, X., Tan, L., Yang, K., Yang, H., et al. (2017). Biocompatibility and neurotoxicity of magnesium alloys potentially used for neural repairs. *Mater. Sci. Eng. C Mater. Biol. Appl.* 78, 1155–1163. <https://doi.org/10.1016/j.msec.2017.04.106>.
- Almansoori, A.A., Ju, K.W., Kim, B., Kim, S.M., Lee, S.-M., and Lee, J.-H. (2018). Hydroxyapatite coated magnesium alloy for peripheral nerve regeneration. *Oral Biol. Res.* 42, 105–113. <https://doi.org/10.21851/obr.42.03.201809.105>.
- Zhang, W., Wang, N., Yang, M., Sun, T., Zhang, J., Zhao, Y., Huo, N., and Li, Z. (2022). Periosteum and development of the tissue-engineered periosteum for guided bone regeneration. *J. Orthop. Translat.* 33, 41–54. <https://doi.org/10.1016/j.jot.2022.01.002>.
- Liu, Y., Long, L., Zhang, F., Hu, X., Zhang, J., Hu, C., Wang, Y., and Xu, J. (2021). Microneedle-mediated vascular endothelial growth factor delivery promotes angiogenesis and functional recovery after stroke. *J. Control. Release* 338, 610–622. <https://doi.org/10.1016/j.jconrel.2021.08.057>.
- Madura, T., Yamashita, T., Kubo, T., Fujitani, M., Hosokawa, K., and Tohyama, M. (2004). Activation of Rho in the injured axons following spinal cord injury. *EMBO Rep.* 5, 412–417. <https://doi.org/10.1038/sj.embor.7400117>.
- Hiraga, A., Kuwabara, S., Doya, H., Kanai, K., Fujitani, M., Taniguchi, J., Arai, K., Mori, M., Hattori, T., and Yamashita, T. (2006). Rho-kinase inhibition enhances axonal regeneration after peripheral nerve injury. *J. Peripher. Nerv. Syst.* 11, 217–224. <https://doi.org/10.1111/j.1529-8027.2006.00091.x>.

30. Kubo, T., Yamaguchi, A., Iwata, N., and Yamashita, T. (2008). The therapeutic effects of Rho-ROCK inhibitors on CNS disorders. *Ther. Clin. Risk Manag.* 4, 605–615. <https://doi.org/10.2147/tcrm.s2907>.
31. Janani, C., and Ranjitha Kumari, B.D. (2015). PPAR gamma gene—a review. *Diabetes Metab. Syndr.* 9, 46–50. <https://doi.org/10.1016/j.dsx.2014.09.015>.
32. Wakino, S., Hayashi, K., Kanda, T., Tatematsu, S., Homma, K., Yoshioka, K., Takamatsu, I., and Saruta, T. (2004). Peroxisome proliferator-activated receptor gamma ligands inhibit Rho/Rho kinase pathway by inducing protein tyrosine phosphatase SHP-2. *Circ. Res.* 95, e45–e55. <https://doi.org/10.1161/01.RES.0000142313.68389.92>.
33. Paintlia, A.S., Paintlia, M.K., Singh, A.K., and Singh, I. (2013). Modulation of Rho-Rock signaling pathway protects oligodendrocytes against cytokine toxicity via PPAR- α -dependent mechanism. *Glia* 61, 1500–1517. <https://doi.org/10.1002/glia.22537>.
34. Rayner, M.L.D., Healy, J., and Phillips, J.B. (2021). Repurposing Small Molecules to Target PPAR- γ as New Therapies for Peripheral Nerve Injuries. *Biomolecules* 11, 1301. <https://doi.org/10.3390/biom11091301>.
35. Patel, H., Giri, P., Patel, P., Singh, S., Gupta, L., Patel, U., Modi, N., Shah, K., Jain, M.R., Srinivas, N.R., and Patel, P. (2018). Preclinical evaluation of saroglitazar magnesium, a dual PPAR- α/γ agonist for treatment of dyslipidemia and metabolic disorders. *Xenobiotica* 48, 1268–1277. <https://doi.org/10.1080/00498254.2017.1413264>.
36. Jamilian, M., Samimi, M., Faraneh, A.E., Aghadavod, E., Shahrzad, H.D., Chamani, M., Mafi, A., and Asemi, Z. (2017). Magnesium supplementation affects gene expression related to insulin and lipid in patients with gestational diabetes. *Magnes. Res.* 30, 71–79. <https://doi.org/10.1684/mrh.2017.0425>.

STAR★METHODS

KEY RESOURCES TABLE

REAGENT or RESOURCE	SOURCE	IDENTIFIER
Chemicals, antibodies, and recombinant proteins		
Magnesium	Henan Yuhang Metal Materials Co., Ltd	NA
Ca-EDTA	EFL Shanghai Mayer Chemical Technology Co., Ltd	NA
KH ₂ PO ₄	Chongqing Yuexiang Chemical Co., Ltd	NA
GelMA	EFL	EFL-GM-30/60/90
GDNF	Sino Biological Inc	80050-R07B
4% Paraformaldehyde	Servicebio	G1101
Hematoxylin	Servicebio	G1005
Eosin	Servicebio	G1005
Masson staining reagent	Servicebio	GP1032
Sirius Red solution	Servicebio	GP1138
Toluidine blue	Servicebio	GP1052
2.5% glutaraldehyde	Servicebio	G1102
Trinton-x 100	Beyotime	ST795
Bovine serum albumin	Meilunbio	MB4219
PBS	Servicebio	G0002
BCA assay kit	Zhonghui Hecai Biotechnology Co., Ltd.	PQ003
NF-200 Rabbit Polyclonal antibody	Proteintech	18934-1-AP
MBP Mouse Monoclonal antibody	Proteintech	66003-1-Ig
P75 Neurotrophin Receptor Rabbit Polyclonal antibody	Proteintech	11733-1-AP
S100 Rabbit Polyclonal antibody	Proteintech	15146-1-AP
PPAR-γ Rabbit Polyclonal antibody	Proteintech	Proteintech
RhoA Rabbit Polyclonal antibody	Selleck	A5651
ROCK Rabbit Polyclonal antibody	Selleck	A5141
GAPDH Rabbit Recombinant mAb	Selleck	A5028
One-Step PAGE Gel Fast preparation kit	Epizyme	PG212
PVDF membrane	Merck Millipore Ltd.	IPVH00010
Tris-buffered saline	Servicebio	G0001
HRP-conjugated goat anti-mouse IgG(H + L)	InCellGenE	SA-10010
HRP-conjugated Goat Anti-Rabbit IgG(H + L)	InCellGenE	SA-10011
Fdbio-Dura ECL Kit	Fdbio science	FD8020
Coralite 488-conjugated Goat Anti-Rabbit IgG(H + L)	Proteintech	SA00013-2
Coralite 594-conjugated Goat Anti-Mouse IgG(H + L)	Proteintech	SA00013-3
Experimental instruments and equipment		
Transmission electron microscopy	Thermo Fisher Scientific Inc	Talos L120C G2
Fluorescence microscope	ZEISS	Axio observer
Biochemical Analyzer	Thermo Fisher Scientific Inc	Sorvall ST 40
Electrophoresis System	Bio-rad	PAC300
Prism V9	GraphPad Software	NA
Image-Pro Plus 6.0	MEDIA CYBERNETICS	NA
ImageJ 1.8	National Institutes of Health	NA
Gene Expression Omnibus (GEO) Database	National Center for Biotechnology Information	GSE243282

RESOURCE AVAILABILITY

Lead contact

Further information and requests for resources and reagents should be directed to and will be fulfilled by the Lead Contact, Xiaoqian Dang (dangxiaoqian@xjtu.edu.cn).

Materials availability

The present study did not generate new unique reagents.

Data and code availability

- Data reported in this paper will be shared by the [lead contact](#) upon request, the RNA seq dataset was available at GEO repository (GSE243282).
- This paper does not report original code.
- Any additional information required to reanalyze the data reported in this paper is available from the [lead contact](#) upon request.

EXPERIMENTAL MODEL AND STUDY PARTICIPANT DETAILS

Rat

All experiments involving rabbits were conducted in accordance with the Guide for the Care and Use of Laboratory Animals of the National Institutes of Health and were approved by the Internal Animal Committee Review Board of the Second Affiliated Hospital of Xi'an Jiaotong University.

SD rats were maintained at the Xi'an Jiaotong University. Male rats (8 weeks) were housed in individual cages with an artificial 12:12 h light:dark cycle at room temperature and fed with normal chow for 2 weeks. Sciatic nerve defect model were made in SD rats.

METHOD DETAILS

Preparation and characterization of GDNF-Gel/HA-Mg nerve conduit

Magnesium ingot (99.99 wt. %, Henan Yuhang Metal Materials Co., Ltd., China) was extruded at a temperature of 220°C to form a Mg rod with a diameter of 15mm. Then, the Mg conduit (length 12mm, inner diameter 2mm, thickness 0.5mm) was prepared using wire cutting. A mixed solution was prepared using a concentration of 0.25 mol/L calcium ethylenediaminetetraacetate (Ca-EDTA) (Shanghai Mayer Chemical Technology Co., Ltd., China) and potassium dihydrogen phosphate (KH₂PO₄) (Chongqing Yuexiang Chemical Co., Ltd., China). The samples were immersed in the mixed solution for liquid-phase deposition to get hydroxyapatite-coated magnesium (HA-Mg) conduit. Gelatin methacryloyl (GelMA) was dissolved in an initiator solution at 60°C–70°C in the dark. Glial cell line-derived neurotrophic factor (GDNF) (Sino Biological Inc., China) was added to obtain GDNF-Gel solution. The HA-Mg nerve conduits were placed in the GDNF-Gel solution, repeatedly pulled and then exposed to 405nm ultraviolet light to crosslink the GDNF-Gel solution into GDNF-Gel gel, thereby obtaining GDNF-Gel/HA-Mg.

The GDNF-Gel/HA-Mg extracts were prepared, and culture with Schwann cells to explored its effects on Schwann cell proliferation, migration, and invasion.

The sciatic nerve defect model in SD rats and implantation of GDNF-Gel/HA-Mg nerve conduit

Twenty-four male adult SD rats were randomly divided into three groups: negative control group (NC group), autograft group (Auto group), and GDNF-Gel/HA-Mg group, with 8 rats in each group. The SD rats were anesthetized, the skin and fascia were sequentially incised to expose the sciatic nerve. Approximately 10 mm of the sciatic nerve was excised using micro scissors. In the NC group, the wound was directly closed without any additional treatment. In the Auto group, under the surgical microscope, the excised autologous sciatic nerve was sutured by perineurial suture to connect the two severed ends. In the GDNF-Gel/HA-Mg group, the GDNF-Gel/HA-Mg nerve conduit was sutured to the sciatic nerve ends using 8-0 sutures, with 2 stitches on each end (Figures 2A and 2B). After suturing, the wound was closed. The rats were housed individually. Each experimental rat received intraperitoneal injections of penicillin twice a day for 7 days and the skin incision was disinfected daily with 75% ethanol for 1 week.

Measurement of sciatic functional index (SFI)

To assess the sciatic nerve function, a pathway leading to the rat's cage was prepared. Prior to the experiment, it is important to allow the animals to be familiar with the environment and train them to pass through the pathway and the cage repeatedly. At 12-week post-surgery, non-toxic dye was applied to the hind paws of the rats. They were then allowed to walk on a pathway covered with white paper, which recorded their footprints. The sciatic functional index (SFI) was calculated using the following formula:

$$\text{SFI} = -38.3 * [(\text{EPL} - \text{NPL}) / \text{NPL}] + 109.5 * [(\text{ETS} - \text{NTS}) / \text{NTS}] + 13.3 * [(\text{EIT} - \text{NIT}) / \text{NIT}] - 8.8$$

PL: Distance from the heel to the third toe; TS: Distance from the first toe to the fifth toe; IT: Distance from the second toe to the fourth toe; E: Surgical side; N: Normal side.

In normal rats, the SFI is 0, while a complete sciatic nerve transection results in an SFI of -100 .

Hematoxylin and eosin (HE) staining

At 12-week post-surgery, after anaesthetization, rats were sacrificed and subjected to routine disinfection. The skin was carefully dissected layer by layer, allowing for visual observation of nerve growth. The sciatic nerve was perfused with saline and 4% paraformaldehyde (Servicebio, China). Following the dissection of the sciatic nerve, it was fixed in paraformaldehyde for 48h. Subsequently, an automatic dehydrator was used for dehydration, and the samples were embedded in paraffin and sectioned.

The slides were placed in a hematoxylin solution (Servicebio, China) for staining for 2–3 min, followed by rinsing with running water. Then, the slides were immersed in eosin solution (Servicebio, China) for 1 min and rinsed with running water. After air-drying, the slides were mounted with neutral gum for microscopic observation and photography.

To assess the biological safety of GDNF-Gel/HA-Mg, heart, liver, spleen, lung, and kidney from different groups were also collected for HE examination to evaluate the changes of pathological structure in major organs.

Masson staining, sirius red staining

After nerve tissue sections were prepared, Masson staining was conducted to observe the growth of nerve fibers. In brief, the sections underwent dewaxing (xylene, 3 times, 10 min each time) and were subsequently immersed sequentially in 100% ethanol for 5 min, 90% ethanol for 2 min, 80% ethanol for 2 min, and 70% ethanol for 2 min. Following this, the sections were rinsed with distilled water for 3 min. Next, they were treated with hematoxylin solution for 10 min, rinsed with running water for 5s, and differentiated with 1% hydrochloric acid ethanol. After rinsing with running water for 2 min, the sections were exposed to Masson's composite staining reagent (Servicebio, China) for 5 min. Following a 10s rinse with running water, the sections were treated with 1% phosphotungstic acid for 2 min, and then directly subjected to aniline blue staining for 5 min. Subsequently, a 1 min treatment with 1% acetic acid was applied, and rapid dehydration was achieved using 95% ethanol to 100% ethanol. Finally, the sections were immersed in xylene three times with 2 min for each time, mounted with neutral gum, then observed and photographed under a microscope. Quantitative measurements were conducted using Image-Pro Plus 6.0.

For Sirius Red staining, the paraffin-embedded sections underwent dewaxing and were washed with water. They were then stained with Sirius Red solution (Servicebio, China) for 8 min, dehydrated with ethanol, cleared with xylene for 5 min, and mounted with neutral gum. The sections were observed and photographed using a polarized light microscopy.

Myelinated nerve fibers and myelin sheath thickness measurement

To evaluate the myelinated nerve fibers, regenerated nerve tissues were obtained from randomly selected SD rats in each group 12 weeks after surgery. The harvested tissues were fixed, dehydrated, and embedded to prepare semi-thin sections. These sections were subsequently stained with toluidine blue (TB) (Servicebio, China) and subjected to quantitative analysis using Image-Pro Plus 6.0 to determine the number of myelinated nerve fibers.

At 12 weeks post-surgery, after anaesthetization, regenerated nerve tissues were harvested from rats. The harvested nerve tissues were initially pre-fixed using a 2.5% glutaraldehyde solution (Servicebio, China). After dehydration through a series of graded ethanol concentrations, the samples were embedded in epoxy resin 618 and prepared as ultrathin sections measuring $1\mu\text{m}$ in thickness. These sections underwent staining with lead citrate and uranyl acetate for transmission electron microscopy (TEM) (Thermo Fisher Scientific Inc., USA) to measure the diameter of the nerve fibers as well as the thickness of the myelin sheath.

Neurophysiology and gastrocnemius muscle wet weight measurement

At 12 weeks post-surgery, randomly selected SD rats from each group were subjected to nerve conduction velocity (NCV) and latency measurements using the BL-420 Biological Function Experiment System. After 12 weeks post-surgery, animals from each group that underwent neurophysiological testing were sacrificed. The gastrocnemius muscle was carefully dissected from the starting point of the femoral condyles to the distal end of the calcaneal tuberosity. The wet weight of the muscle was accurately measured.

Immunofluorescence (IF)

The nerve tissue sections were washed 3 times with PBS for 5 min each. After fixation, the sections were incubated with 0.5% Triton X-100 (Beyotime Biotechnology, China) for 5 min, followed by 3 washes with PBS for 5 min each. Subsequently, the sections were blocked with 5% bovine serum albumin (BSA) (Meilunbio, China) at room temperature for 30 min. Primary antibodies were added and incubated overnight at 4°C . The primary antibodies used in this study including neurofilament-200 (NF-200) Rabbit Polyclonal antibody (1:200; Proteintech, China), myelin basic protein (MBP) Mouse Monoclonal antibody (1:200; Proteintech, China), P75 Neurotrophin Receptor Rabbit Polyclonal antibody (1:300; Proteintech, China), S100 Rabbit Polyclonal antibody (1:100; Proteintech, China), and peroxisome proliferator-activated receptor gamma (PPAR- γ) Rabbit Polyclonal antibody (1:300; Proteintech, China). The next day, the sections were washed 3 times with PBS for 5 min each. CoraLite 488-conjugated Goat Anti-Rabbit IgG(H + L) or CoraLite 594-conjugated Goat Anti-Mouse IgG(H + L) (1:1000; Proteintech, China), were added and incubated at room temperature for 2 h in the dark. After three washes with PBS for 5 min each, the sections were stained with DAPI for 10 min. Following three additional washes with PBS, the sections were mounted with antifade mounting agent

(Meilunbio, China). The sections were then observed and photographed under a fluorescence microscope (ZEISS, Germany), and quantitative measurements were performed by Image-Pro Plus 6.0.

Quantitative real-time PCR (qPCR)

The regenerated nerve tissues were subjected to RNA extraction by the RNAiso Puls Reagent (Takara, Dalian, Liaoning, China) following the manufacturer's instructions. To generate the strand cDNA, the RNA samples were subjected to reverse transcription using the StarScript First-strand cDNA Synthesis Mix kit (Genstar, Beijing, China). The expression of PPAR- γ , RhoA and ROCK1 were quantified using gene-specific prim (Table S1) and the SYBR Green PCR Master Mix (Yeasen, Shanghai, China). Moreover, GAPDH served as the endogenous control gene. All qPCR analyses were conducted using a Bio-rad Real-time PCR instrument (Bio-rad, Shanghai, China). The results of the q-PCR analyses were determined by the $2^{-\Delta\Delta CT}$ method.

Western blotting

Radioimmunoprecipitation assay (RIPA) lysis buffer (Boster Biological Technology co.ltd, China) was used to extract proteins from the sciatic nerve tissues of rats harvested from each group. The protein concentration was determined using the BCA assay kit (Zhonghui Hecai Biotechnology Co., Ltd., China). The proteins were separated by SDS-PAGE (Epizyme Biotech, China), transferred to PVDF membrane (Merck Millipore Ltd., Germany), and then blocked with 5% skim milk. PPAR Gamma Rabbit Polyclonal antibody (1:500; Proteintech, China), RhoA Rabbit Polyclonal antibody (1:1000; Selleck, USA), Rho-associated kinase (ROCK) Rabbit Polyclonal antibody (1:500; Selleck, USA), and GAPDH Rabbit Monoclonal antibody (1:50000; Selleck, USA) were added and incubated overnight at 4°C. The membrane was washed three times with Tris-buffered saline with Tween (TBST) (Servicebio, China), 10 min each time. HRP-conjugated goat anti-rabbit or goat anti-mouse IgG (1:10000; InCellGenE, USA) were added and incubated at room temperature for 2 h. After three washes with TBST, 10 min each time, enhanced chemiluminescence substrate (ECL) was used for signal detection by Bio-Rad automated chemiluminescence imaging system. The relative expression levels of the target proteins were determined by calculating the grayscale ratio between the target proteins and GAPDH. Quantitative measurements were performed using ImageJ 1.8.

RNA-seq and bioinformatics analysis

Total RNA was extracted using Trizol reagent kit (Invitrogen, Carlsbad, CA, USA) according to the manufacturer's protocol. RNA quality was assessed on an Agilent 2100 Bioanalyzer (Agilent Technologies, Palo Alto, CA, USA) and checked using RNase free agarose gel electrophoresis. After total RNA was extracted, eukaryotic mRNA was enriched by Oligo(dT) beads. Then the enriched mRNA was fragmented into short fragments using fragmentation buffer and reversly transcribed into cDNA by using NEBNext Ultra RNA Library Prep Kit for Illumina (NEB #7530, New England Biolabs, Ipswich, MA, USA). The purified double-stranded cDNA fragments were end repaired, A base added, and ligated to Illumina sequencing adapters. The ligation reaction was purified with the AMPure XP Beads (1.0X). Ligated fragments were subjected to size selection by agarose gel electrophoresis and polymerase chain reaction (PCR) amplified. The resulting cDNA library was sequenced using Illumina Novaseq6000 by Gene Denovo Biotechnology Co. (Guangzhou, China). To get high quality clean reads, reads were further filtered by fastp (version 0.18.0). The genes with the parameter of false discovery rate (FDR) below 0.05 and absolute fold change ≥ 2 were considered differentially expressed genes. Principal Component Analysis (PCA), Cluster analysis, GO Enrichment Analysis, KEGG Pathway Enrichment Analysis and Gene Set Enrichment Analysis (GSEA) were then performed.

Biological safety assessment

To assess the effect of GDNF-Gel/HA-Mg on the functions of major organs, blood samples from different groups were collected by EDTA blood collection vacutainer, then centrifuge at 3000rpm for 20 min at 4°C, the supernatants were collect and stored at -80°C. The myocardial enzymes, transaminases, and renal function were detected by Biochemical Analyzer according to the manufacturer's instructions.

QUANTIFICATION AND STATISTICAL ANALYSIS

Graphpad Prism 9.0 was utilized for all statistical analyses. Continuous data conforming to a normal distribution were expressed as mean \pm standard deviation. Statistical distinctions between groups were assessed through one-way analysis of variance (ANOVA), followed by Bonferroni-t test for statistical analysis between two groups. A p-value < 0.05 denoted statistical significance.